1

The Wireless Channel: Propagation and Fading

The performance of wireless communication systems is mainly governed by the wireless channel environment. As opposed to the typically static and predictable characteristics of a wired channel, the wireless channel is rather dynamic and unpredictable, which makes an exact analysis of the wireless communication system often difficult. In recent years, optimization of the wireless communication system has become critical with the rapid growth of mobile communication services and emerging broadband mobile Internet access services. In fact, the understanding of wireless channels will lay the foundation for the development of high performance and bandwidth-efficient wireless transmission technology.

In wireless communication, radio propagation refers to the behavior of radio waves when they are propagated from transmitter to receiver. In the course of propagation, radio waves are mainly affected by three different modes of physical phenomena: reflection, diffraction, and scattering [1,2]. *Reflection* is the physical phenomenon that occurs when a propagating electromagnetic wave impinges upon an object with very large dimensions compared to the wavelength, for example, surface of the earth and building. It forces the transmit signal power to be reflected back to its origin rather than being passed all the way along the path to the receiver. *Diffraction* refers to various phenomena that occur when the radio path between the transmitter and receiver is obstructed by a surface with sharp irregularities or small openings. It appears as a bending of waves around the small obstacles and spreading out of waves past small openings. The secondary waves generated by diffraction are useful for establishing a path between the transmitter and receiver, even when a line-of-sight path is not present. Scattering is the physical phenomenon that forces the radiation of an electromagnetic wave to deviate from a straight path by one or more local obstacles, with small dimensions compared to the wavelength. Those obstacles that induce scattering, such as foliage, street signs, and lamp posts, are referred to as the scatters. In other words, the propagation of a radio wave is a complicated and less predictable process that is governed by reflection, diffraction, and scattering, whose intensity varies with different environments at different instances.

A unique characteristic in a wireless channel is a phenomenon called 'fading,' the variation of the signal amplitude over time and frequency. In contrast with the additive noise as the most

MIMO-OFDM Wireless Communications with MATLAB® Yong Soo Cho, Jaekwon Kim, Won Young Yang and Chung G. Kang

common source of signal degradation, fading is another source of signal degradation that is characterized as a non-additive signal disturbance in the wireless channel. Fading may either be due to multipath propagation, referred to as multi-path (induced) fading, or to shadowing from obstacles that affect the propagation of a radio wave, referred to as shadow fading.

The fading phenomenon in the wireless communication channel was initially modeled for HF (High Frequency, 3∼30 MHz), UHF (Ultra HF, 300∼3000 GHz), and SHF (Super HF, 3∼30 GHz) bands in the 1950s and 1960s. Currently, the most popular wireless channel models have been established for 800MHz to 2.5 GHz by extensive channel measurements in the field. These include the ITU-R standard channel models specialized for a single-antenna communication system, typically referred to as a SISO (Single Input Single Output) communication, over some frequency bands. Meanwhile, spatial channel models for a multi-antenna communication system, referred to as the MIMO (Multiple Input Multiple Output) system, have been recently developed by the various research and standardization activities such as IEEE 802, METRA Project, 3GPP/3GPP2, and WINNER Projects, aiming at high-speed wireless transmission and diversity gain.

The fading phenomenon can be broadly classified into two different types: *large-scale fading* and *small-scale fading*. Large-scale fading occurs as the mobile moves through a large distance, for example, a distance of the order of cell size [1]. It is caused by path loss of signal as a function of distance and shadowing by large objects such as buildings, intervening terrains, and vegetation. Shadowing is a slow fading process characterized by variation of median path loss between the transmitter and receiver in fixed locations. In other words, large-scale fading is characterized by average path loss and shadowing. On the other hand, small-scale fading refers to rapid variation of signal levels due to the constructive and destructive interference of multiple signal paths (multi-paths) when the mobile station moves short distances. Depending on the relative extent of a multipath, frequency selectivity of a channel is characterized (e.g., by frequency-selective or frequency flat) for small-scaling fading. Meanwhile, depending on the time variation in a channel due to mobile speed (characterized by the Doppler spread), short-term fading can be classified as either fast fading or slow fading. Figure 1.1 classifies the types of fading channels.

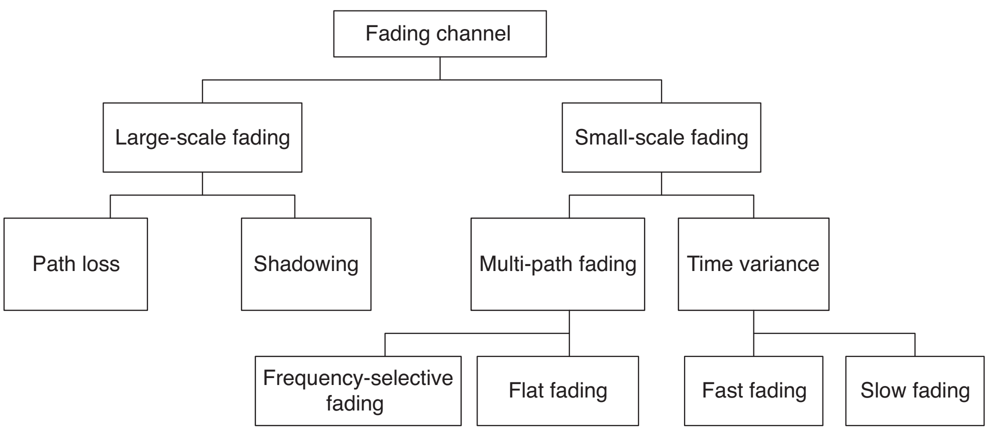

Figure 1.1 Classification of fading channels.

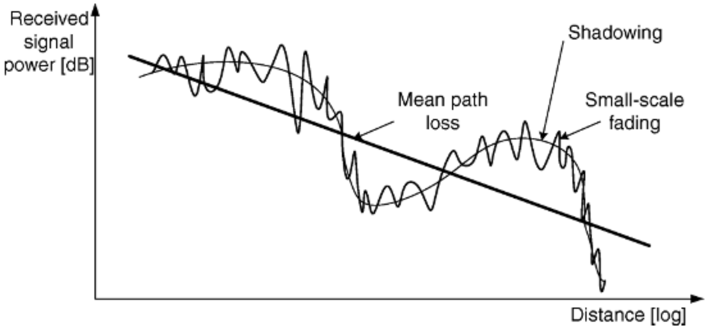

Figure 1.2 Large-scale fading vs. small-scale fading.

The relationship between large-scale fading and small-scale fading is illustrated in Figure 1.2. Large-scale fading is manifested by the mean path loss that decreases with distance and shadowing that varies along the mean path loss. The received signal strength may be different even at the same distance from a transmitter, due to the shadowing caused by obstacles on the path. Furthermore, the scattering components incur small-scale fading, which finally yields a short-term variation of the signal that has already experienced shadowing.

Link budget is an important tool in the design of radio communication systems. Accounting for all the gains and losses through the wireless channel to the receiver, it allows for predicting the received signal strength along with the required power margin. Path loss and fading are the two most important factors to consider in link budget. Figure 1.3 illustrates a link budget that is affected by these factors. The mean path loss is a deterministic factor that can be predicted with the distance between the transmitter and receiver. On the contrary, shadowing and small-scale

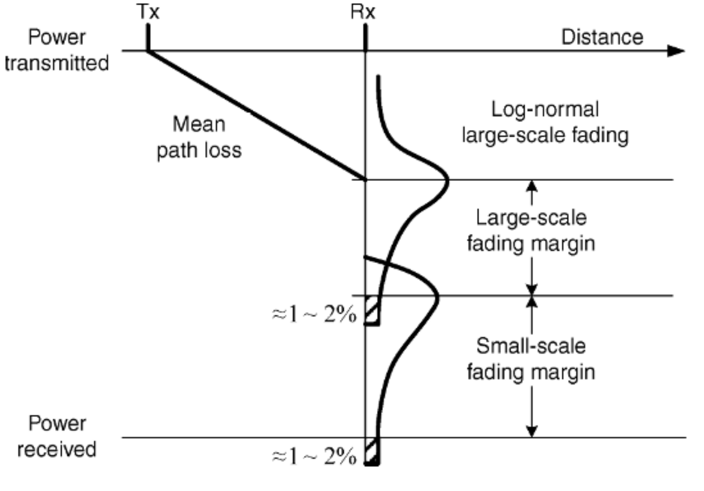

Figure 1.3 Link budget for the fading channel [3]. (© 1994 IEEE. Reproduced from Greenwood, D. and Hanzo, L., "Characterization of mobile radio channels," in *Mobile Radio Communications*, R. Steele (ed.), pp. 91–185, © 1994, with permission from Institute of Electrical and Electronics Engineers (IEEE).)

fading are random phenomena, which means that their effects can only be predicted by their probabilistic distribution. For example, shadowing is typically modeled by a log-normal distribution.

Due to the random nature of fading, some power margin must be added to ensure the desired level of the received signal strength. In other words, we must determine the margin that warrants the received signal power beyond the given threshold within the target rate (e.g., 98–99%) in the design. As illustrated in Figure 1.3, large-scale and small-scale margins must be set so as to maintain the outage rate within 1~2%, which means that the received signal power must be below the target design level with the probability of 0.02 or less [3]. In this analysis, therefore, it is essential to characterize the probabilistic nature of shadowing as well as the path loss.

In this chapter, we present the specific channel models for large-scale and small-scale fading that is required for the link budget analysis.

1.1 Large-Scale Fading

1.1.1 General Path Loss Model

The free-space propagation model is used for predicting the received signal strength in the line-of-sight (LOS) environment where there is no obstacle between the transmitter and receiver. It is often adopted for the satellite communication systems. Let d denote the distance in meters between the transmitter and receiver. When non-isotropic antennas are used with a transmit gain of G_t and a receive gain of G_r, the received power at distance d, $P_r(d)$, is expressed by the well-known Friis equation [4], given as

$$P_r(d) = \frac{P_t G_t G_r \lambda^2}{(4\pi)^2 d^2 L} \tag{1.1}$$

where P_t represents the transmit power (watts), λ is the wavelength of radiation (m), and L is the system loss factor which is independent of propagation environment. The system loss factor represents overall attenuation or loss in the actual system hardware, including transmission line, filter, and antennas. In general, $L > 1$, but $L = 1$ if we assume that there is no loss in the system hardware. It is obvious from Equation (1.1) that the received power attenuates exponentially with the distance d. The free-space path loss, $PL_F(d)$, without any system loss can be directly derived from Equation (1.1) with $L = 1$ as

$$PL_F(d)[dB] = 10\log\left(\frac{P_t}{P_r}\right) = -10\log\left(\frac{G_t G_r \lambda^2}{(4\pi)^2 d^2}\right) \tag{1.2}$$

Without antenna gains (i.e., $G_t = G_r = 1$), Equation (1.2) is reduced to

$$PL_F(d)[dB] = 10\log\left(\frac{P_t}{P_r}\right) = 20\log\left(\frac{4\pi d}{\lambda}\right) \tag{1.3}$$

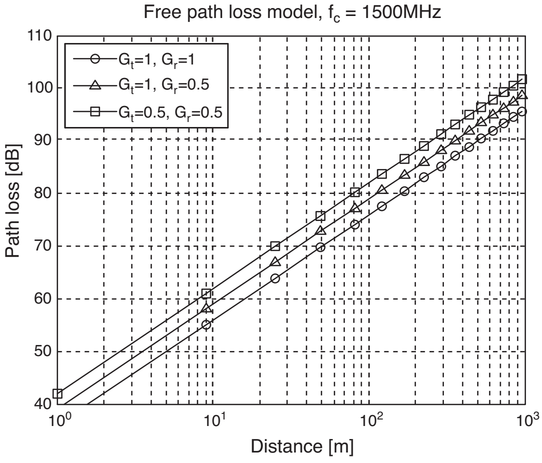

Figure 1.4 Free-space path loss model.

Figure 1.4 shows the free-space path loss at the carrier frequency of $f_c = 1.5\,\text{GHz}$ for different antenna gains as the distance varies. It is obvious that the path loss increases by reducing the antenna gains. As in the aforementioned free-space model, the average received signal in all the other actual environments decreases with the distance between the transmitter and receiver, d, in a logarithmic manner. In fact, a more generalized form of the path loss model can be constructed by modifying the free-space path loss with the path loss exponent n that varies with the environments. This is known as the log-distance path loss model, in which the path loss at distance d is given as

$$PL_{LD}(d)[dB] = PL_F(d_0) + 10n\log\left(\frac{d}{d_0}\right) \tag{1.4}$$

where d_0 is a reference distance at which or closer to the path loss inherits the characteristics of free-space loss in Equation (1.2). As shown in Table 1.1, the path loss exponent can vary from 2 to 6, depending on the propagation environment. Note that $n = 2$ corresponds to the free space. Moreover, n tends to increase as there are more obstructions. Meanwhile, the reference distance

Table 1.1 Path loss exponent [2].

Environment	Path loss exponent (n)
Free space	2
Urban area cellular radio	2.7–3.5
Shadowed urban cellular radio	3–5
In building line-of-sight	1.6–1.8
Obstructed in building	4–6
Obstructed in factories	2–3

(Rappaport, Theodore S., *Wireless Communications: Principles and Practice*, 2nd Edition, © 2002, pg. 76. Reprinted by permission of Pearson Education, Inc., Upper Saddle River, New Jersey.)

d_0 must be properly determined for different propagation environments. For example, d_0 is typically set as 1 km for a cellular system with a large coverage (e.g., a cellular system with a cell radius greater than 10 km). However, it could be 100 m or 1 m, respectively, for a macro-cellular system with a cell radius of 1km or a microcellular system with an extremely small radius [5].

Figure 1.5 shows the log-distance path loss by Equation (1.5) at the carrier frequency of $f_c = 1.5$ GHz. It is clear that the path loss increases with the path loss exponent n. Even if the distance between the transmitter and receiver is equal to each other, every path may have different path loss since the surrounding environments may vary with the location of the receiver in practice. However, all the aforementioned path loss models do not take this particular situation into account. A *log-normal* shadowing model is useful when dealing with a more realistic situation. Let X_σ denote a Gaussian random variable with a zero mean and a standard deviation of σ. Then, the log-normal shadowing model is given as

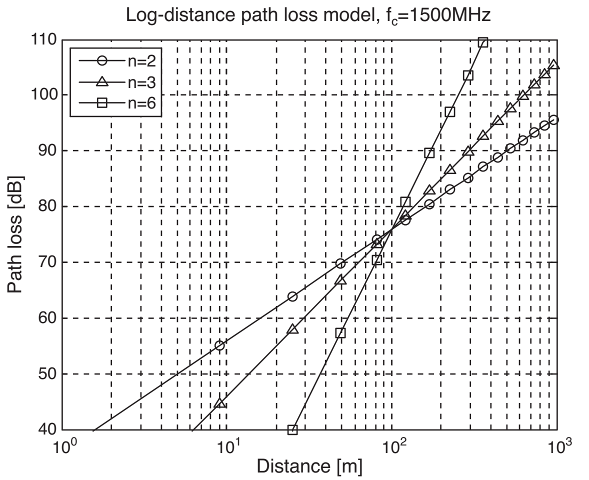

Figure 1.5 Log-distance path loss model.

$$PL(d)[dB] = \overline{PL}(d) + X_\sigma = PL_F(d_0) + 10n\log\left(\frac{d}{d_0}\right) + X_\sigma \tag{1.5}$$

In other words, this particular model allows the receiver at the same distance d to have a different path loss, which varies with the random shadowing effect X_σ. Figure 1.6 shows the path loss that follows the log-normal shadowing model at $f_c = 1.5$ GHz with $\sigma = 3$ dB and $n = 2$. It clearly illustrates the random effect of shadowing that is imposed on the deterministic nature of the log-distance path loss model.

Note that the path loss graphs in Figures 1.4–1.6 are obtained by running Program 1.3 (“plot_PL_general.m”), which calls Programs 1.1 (“PL_free”) and 1.2 (“PL_logdist_or_norm”) to compute the path losses by using Equation (1.2), Equation (1.3), Equation (1.4), and Equation (1.5), respectively.

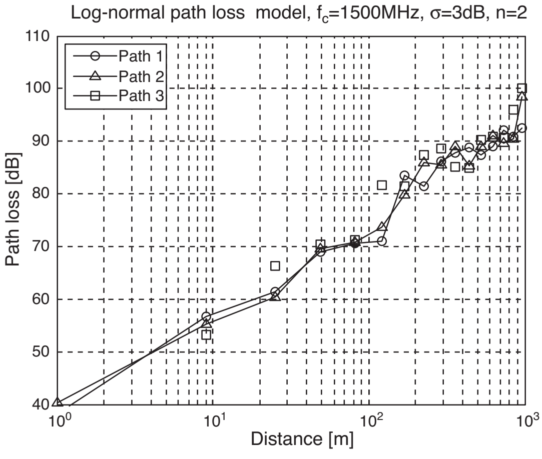

Figure 1.6 Log-normal shadowing path loss model.

MATLAB® Programs: Generalized Path Loss Model

Program 1.1 "PL_logdist_or_norm" for log-distance/normal shadowing path loss model

```
function PL=PL_logdist_or_norm(fc,d,d0,n,sigma)
% Log-distance or Log-normal shadowing path loss model
% Inputs:    fc     : Carrier frequency[Hz]
%            d      : Distance between base station and mobile station[m]
%            d0     : Reference distance[m]
%            n      : Path loss exponent
%            sigma  : Variance[dB]
lamda=3e8/fc; PL= -20*log10(lamda/(4*pi*d0))+10*n*log10(d/d0); % Eq.(1.4)
if nargin>4, PL = PL + sigma*randn(size(d));   end  % Eq.(1.5)
```

Program 1.2 "PL_free" for free-space path loss model

```
function PL=PL_free(fc,d,Gt,Gr)
% Free Space Path Loss Model
% Inputs: fc    : Carrier frequency[Hz]
%         d     : Distance between base station and mobile station[m]
%         Gt/Gr : Transmitter/Receiver gain
% Output: PL    : Path loss[dB]
lamda = 3e8/fc; tmp = lamda./(4*pi*d);
if nargin>2, tmp = tmp*sqrt(Gt); end
if nargin>3, tmp = tmp*sqrt(Gr); end
PL = -20*log10(tmp); % Eq.(1.2)/(1.3)
```

Program 1.3 "plot_PL_general.m" to plot the various path loss models

```
% plot_PL_general.m
clear, clf
fc=1.5e9; d0=100; sigma=3; distance=[1:2:31].^2;
Gt=[1 1 0.5]; Gr=[1 0.5 0.5]; Exp=[2 3 6];
for k=1:3
   y_Free(k,:)=PL_free(fc,distance,Gt(k),Gr(k));
   y_logdist(k,:)=PL_logdist_or_norm(fc,distance,d0,Exp(k));
   y_lognorm(k,:)=PL_logdist_or_norm(fc,distance,d0,Exp(1),sigma);
end
subplot(131), semilogx(distance,y_Free(1,:),'k-o', distance,y_Free(2,:),
 'k-^', distance,y_Free(3,:),'k-s'), grid on, axis([1 1000 40 110]),
title(['Free Path-loss Model, f_c=',num2str(fc/1e6),'MHz'])
xlabel('Distance[m]'), ylabel('Path loss[dB]')
legend('G_t=1, G_r=1','G_t=1, G_r=0.5','G_t=0.5, G_r=0.5',2)
subplot(132)
semilogx(distance,y_logdist(1,:),'k-o', distance,y_logdist(2,:),'k-^',
 distance,y_logdist(3,:),'k-s'), grid on, axis([1 1000 40 110]),
title(['Log-distance Path-loss Model, f_c=',num2str(fc/1e6),'MHz'])
xlabel('Distance[m]'), ylabel('Path loss[dB]'),
legend('n=2','n=3','n=6',2)
subplot(133), semilogx(distance,y_lognorm(1,:),'k-o', distance,y_lognorm
 (2,:),'k-^', distance,y_lognorm(3,:),'k-s')
grid on, axis([1 1000 40 110]), legend('path 1','path 2','path 3',2)
title(['Log-normal Path-loss Model, f_c=',num2str(fc/1e6),'MHz,
 ', '\sigma=', num2str(sigma), 'dB, n=2'])
xlabel('Distance[m]'), ylabel('Path loss[dB]')
```

1.1.2 Okumura/Hata Model

The Okumura model has been obtained through extensive experiments to compute the antenna height and coverage area for mobile communication systems [6]. It is one of the most frequently adopted path loss models that can predict path loss in an urban area. This particular model mainly covers the typical mobile communication system characteristics with a frequency band of 500–1500 MHz, cell radius of 1–100 km, and an antenna height of 30 m to 1000 m. The path loss at distance d in the Okumura model is given as

$$PL_{Ok}(d)[dB] = PL_F + A_{MU}(f,d) - G_{Rx} - G_{Tx} + G_{AREA} \tag{1.6}$$

where $A_{MU}(f,d)$ is the medium attenuation factor at frequency f, G_{Rx} and G_{Tx} are the antenna gains of Rx and Tx antennas, respectively, and G_{AREA} is the gain for the propagation environment in the specific area. Note that the antenna gains, G_{Rx} and G_{Tx}, are merely a function of the antenna height, without other factors taken into account like an antenna pattern. Meanwhile, $A_{MU}(f,d)$ and G_{AREA} can be referred to by the graphs that have been obtained empirically from actual measurements by Okumura [6].

The Okumura model has been extended to cover the various propagation environments, including urban, suburban, and open area, which is now known as the Hata model [7]. In fact, the Hata model is currently the most popular path loss model. For the height of transmit antenna, h_{TX}[m], and the carrier frequency of f_c[MHz], the path loss at distance d [m] in an urban area is given by the Hata model as

$$PL_{Hata,U}(d)[dB] = 69.55 + 26.16\log f_c - 13.82\log h_{TX} - C_{RX} + (44.9 - 6.55\log h_{TX})\log d \quad (1.7)$$

where C_{RX} is the correlation coefficient of the receive antenna, which depends on the size of coverage. For small to medium-sized coverage, C_{RX} is given as

$$C_{Rx} = 0.8 + (1.1\log f_c - 0.7)h_{Rx} - 1.56\log f_c \quad (1.8)$$

where h_{RX} [m] is the height of transmit antenna. For large-sized coverage, C_{RX} depends on the range of the carrier frequency, for example,

$$C_{RX} = \begin{cases} 8.29(\log(1.54h_{RX}))^2 - 1.1 & \text{if } 150\,\text{MHz} \le f_c \le 200\,\text{MHz} \\ 3.2(\log(11.75h_{RX}))^2 - 4.97 & \text{if } 200\,\text{MHz} \le f_c \le 1500\,\text{MHz} \end{cases} \quad (1.9)$$

Meanwhile, the path loss at distance d in suburban and open areas are respectively given by the Hata model as

$$PL_{Hata,SU}(d)[dB] = PL_{Hata,U}(d) - 2\left(\log\frac{f_c}{28}\right)^2 - 5.4 \quad (1.10)$$

and

$$PL_{Hata,O}(d)[dB] = PL_{Hata,U}(d) - 4.78(\log f_c)^2 + 18.33\log f_c - 40.97 \quad (1.11)$$

Figure 1.7 presents the path loss graphs for the three different environments – urban, suburban, and open areas – given by the models in Equations (1.7), (1.10), and (1.11), respectively. It is clear that the urban area gives the most significant path loss as compared to the other areas,

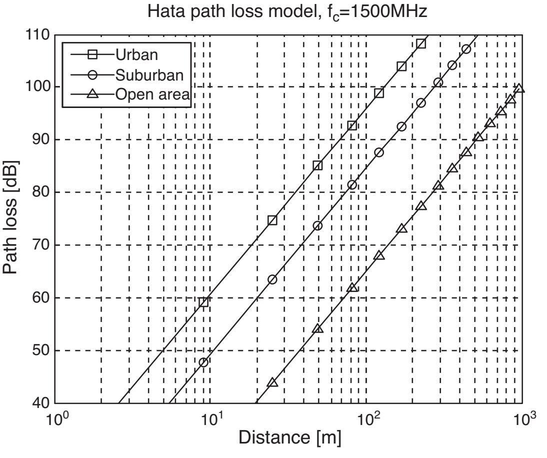

Figure 1.7 Hata path loss model.

simply due to the dense obstructions observed in the urban area. Note that these path loss graphs in Figure 1.7 are obtained by running Program 1.4 (“plot_PL_Hata.m”), which calls Program 1.5 (”PL_Hata”) to compute the path losses for various propagation environments by using Equations (1.7)∼(1.11).

MATLAB® Programs: Hata Path Loss Model

Program 1.4 “plot_PL_Hata.m” to plot the Hata path loss model

```
% plot_PL_Hata.m
clear, clf
fc=1.5e9; htx=30; hrx=2; distance=[1:2:31].^2;
y_urban=PL_Hata(fc,distance,htx,hrx,'urban');
y_suburban=PL_Hata(fc,distance,htx,hrx,'suburban');
y_open=PL_Hata(fc,distance,htx,hrx,'open');
semilogx(distance,y_urban,'k-s', distance,y_suburban,'k-o', distance,
 y_open,'k-^')
title(['Hata PL model, f_c=',num2str(fc/1e6),'MHz'])
xlabel('Distance[m]'), ylabel('Path loss[dB]')
legend('urban','suburban','open area',2), grid on, axis([1 1000 40 110])
```

Program 1.5 “PL_Hata” for Hata path loss model

```
function PL=PL_Hata(fc,d,htx,hrx,Etype)
% Inputs: fc    : Carrier frequency[Hz]
%         d     : Distance between base station and mobile station[m]
%         htx   : Height of transmitter[m]
%         hrx   : Height of receiver[m]
%         Etype : Environment type('urban','suburban','open')
% Output: PL    : path loss[dB]
if nargin<5, Etype = 'URBAN'; end
fc=fc/(1e6);
if fc>=150&&fc<=200, C_Rx = 8.29*(log10(1.54*hrx))^2 - 1.1;
  elseif fc>200, C_Rx = 3.2*(log10(11.75*hrx))^2 - 4.97; % Eq.(1.9)
  else C_Rx = 0.8+(1.1*log10(fc)-0.7)*hrx-1.56*log10(fc); % Eq.(1.8)
end
PL = 69.55 +26.16*log10(fc) -13.82*log10(htx) -C_Rx ...
     +(44.9-6.55*log10(htx))*log10(d/1000); % Eq.(1.7)
EType = upper(Etype);
if EType(1)=='S', PL = PL -2*(log10(fc/28))^2 -5.4; % Eq.(1.10)
  elseif EType(1)=='O'
    PL=PL+(18.33-4.78*log10(fc))*log10(fc)-40.97; % Eq.(1.11)
end
```

1.1.3 IEEE 802.16d Model

IEEE 802.16d model is based on the log-normal shadowing path loss model. There are three different types of models (Type A, B, and C), depending on the density of obstruction between the transmitter and receiver (in terms of tree densities) in a macro-cell suburban area. Table 1.2 describes these three different types of models in which ART and BRT stand for Above-Roof-Top and Below-Roof-Top. Referring to [8–11], the IEEE 802.16d path loss model is given as

$$PL_{802.16}(d)[dB] = PL_F(d_0) + 10\gamma \log_{10}\left(\frac{d}{d_0}\right) + C_f + C_{RX} \quad \text{for} \quad d > d_0 \tag{1.12}$$

Table 1.2 Types of IEEE 802.16d path loss models.

Type	Description
A	Macro-cell suburban, ART to BRT for hilly terrain with moderate-to-heavy tree densities
B	Macro-cell suburban, ART to BRT for intermediate path loss condition
C	Macro-cell suburban, ART to BRT for flat terrain with light tree densities

In Equation (1.12), $d_0 = 100\,m$ and $\gamma = a - bh_{Tx} + c/h_{TX}$ where a, b, and c are constants that vary with the types of channel models as given in Table 1.3, and h_{TX} is the height of transmit antenna (typically, ranged from 10 m to 80 m). Furthermore, C_f is the correlation coefficient for the carrier frequency f_c [MHz], which is given as

$$C_f = 6 \log_{10}(f_c/2000) \tag{1.13}$$

Table 1.3 Parameters for IEEE 802.16d type A, B, and C models.

Parameter	Type A	Type B	Type C
a	4.6	4	3.6
b	0.0075	0.0065	0.005
c	12.6	17.1	20

Meanwhile, C_{RX} is the correlation coefficient for the receive antenna, given as

$$C_{RX} = \begin{cases} -10.8 \log_{10}(h_{RX}/2) & \text{for Type A and B} \\ -20 \log_{10}(h_{RX}/2) & \text{for Type C} \end{cases} \tag{1.14}$$

or

$$C_{RX} = \begin{cases} -10 \log_{10}(h_{RX}/3) & \text{for } h_{RX} \leq 3m \\ -20 \log_{10}(h_{RX}/3) & \text{for } h_{RX} > 3m \end{cases} \tag{1.15}$$

The correlation coefficient in Equation (1.14) is based on the measurements by AT&T while the one in Equation (1.15) is based on the measurements by Okumura.

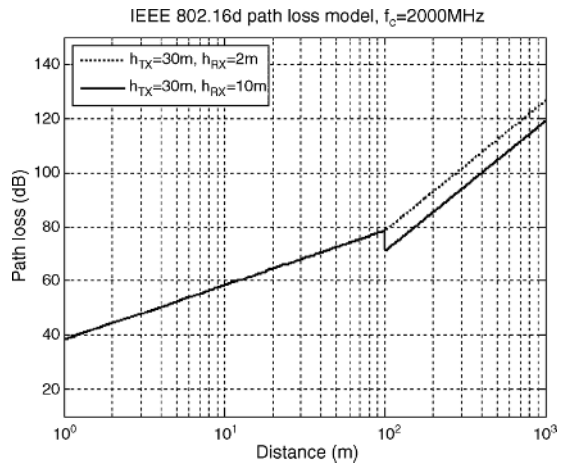

Figure 1.8 IEEE 802.16d path loss model.

Figure 1.8 shows the path loss by the IEEE 802.16d model at the carrier frequency of 2 GHz, as the height of the transmit antenna is varied and the height of the transmit antenna is fixed at 30 m. Note that when the height of the transmit antenna is changed from 2 m to 10 m, there is a discontinuity at the distance of 100 m, causing some inconsistency in the prediction of the path loss. For example, the path loss at the distance of 101 m is larger than that at the distance of 99 m by 8dB, even without a shadowing effect in the model. It implies that a new reference distance d_0' must be defined to modify the existing model [9]. The new reference distance d_0' is determined by equating the path loss in Equation (1.12) to the free-space loss in Equation (1.3), such that

$$20\log_{10}\left(\frac{4\pi d_0'}{\lambda}\right) = 20\log_{10}\left(\frac{4\pi d_0'}{\lambda}\right) + 10\gamma\log_{10}\left(\frac{d_0'}{d_0}\right) + C_f + C_{RX} \qquad (1.16)$$

Solving Equation (1.16) for d_0', the new reference distance is found as

$$d_0' = d_0 10^{-\frac{C_f + C_{RX}}{10\gamma}} \qquad (1.17)$$

Substituting Equation (1.17) into Equation (1.12), a modified IEEE 802.16d model follows as

$$PL_{M802.16}(d)[dB] = \begin{cases} 20\log_{10}\left(\frac{4\pi d}{\lambda}\right) & \text{for } d \le d_0' \\ 20\log_{10}\left(\frac{4\pi d_0'}{\lambda}\right) + 10\gamma\log_{10}\left(\frac{d}{d_0}\right) + C_f + C_{RX} & \text{for } d > d_0' \end{cases} \qquad (1.18)$$

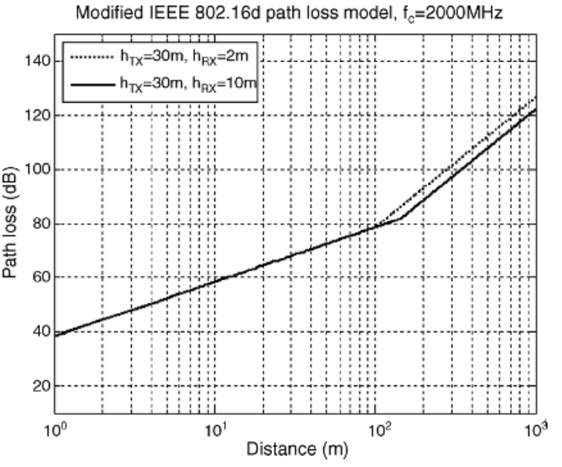

Figure 1.9 Modified IEEE 802.16d path loss model.

Figure 1.9 shows the path loss by the modified IEEE 802.16d model in Equation (1.18), which has been plotted by running the Program 1.7 (“plot_PL_IEEE80216d.m”), which calls Program 1.6 (“PL_IEEE80216d”). Discontinuity is no longer shown in this modified model, unlike the one in Figure 1.8.

MATLAB® Programs: IEEE 802.16d Path Loss Model

Program 1.6 “PL_IEEE80216d” for IEEE 802.16d path loss model

```
function PL=PL_IEEE80216d(fc,d,type,htx,hrx,corr_fact,mod)
% IEEE 802.16d model
% Inputs
%      fc        : Carrier frequency
%      d         : Distance between base and terminal
%      type      : selects 'A', 'B', or 'C'
%      htx       : Height of transmitter
%      hrx       : Height of receiver
%      corr_fact : If shadowing exists, set to 'ATnT' or 'Okumura'.
%                    Otherwise, 'NO'
%      mod       : set to 'mod' to obtain modified IEEE 802.16d model
% Output
%      PL : path loss[dB]
Mod='UNMOD';
if nargin>6, Mod=upper(mod); end
if nargin==6&&corr_fact(1)=='m', Mod='MOD'; corr_fact='NO';
  elseif nargin<6, corr_fact='NO';
    if nargin==5&&hrx(1)=='m', Mod='MOD'; hrx=2;
      elseif nargin<5, hrx=2;
        if nargin==4&&htx(1)=='m', Mod='MOD'; htx=30;
```

```
        elseif nargin<4, htx=30;
         if nargin==3&&type(1)=='m', Mod='MOD'; type='A';
           elseif nargin<3, type='A';
         end
       end
    end
end
d0 = 100;
Type = upper(type);
if Type~='A' && Type~='B' &&Type~='C'
  disp('Error: The selected type is not supported'); return;
end
switch upper(corr_fact)
  case 'ATNT',    PLf=6*log10(fc/2e9);                       % Eq.(1.13)
                  PLh=-10.8*log10(hrx/2);                    % Eq.(1.14)
  case 'OKUMURA', PLf=6*log10(fc/2e9);                       % Eq.(1.13)
                    if hrx<=3, PLh=-10*log10(hrx/3);         % Eq.(1.15)
                      else PLh=-20*log10(hrx/3);
                    end
  case 'NO',      PLf=0; PLh=0;
end
if Type=='A',     a=4.6; b=0.0075; c=12.6; % Eq.(1.3)
  elseif Type=='B', a=4; b=0.0065; c=17.1;
  else    a=3.6; b=0.005; c=20;
end
lamda=3e8/fc; gamma=a-b*htx+c/htx; d0_pr=d0;                 % Eq.(1.12)
if Mod(1)=='M'
  d0_pr=d0*10^-((PLf+PLh)/(10*gamma));                       % Eq.(1.17)
end
A = 20*log10(4*pi*d0_pr/lamda) + PLf + PLh;
for k=1:length(d)
  if d(k)>d0_pr, PL(k) = A + 10*gamma*log10(d(k)/d0);       % Eq.(1.18)
    else PL(k) = 20*log10(4*pi*d(k)/lamda);
  end
end
```

Program 1.7 "plot_PL_IEEE80216d.m" to plot the IEEE 802.16d path loss model

```
% plot_PL_IEEE80216d.m
clear, clf, clc
fc=2e9; htx=[30 30]; hrx=[2 10]; distance=[1:1000];
for k=1:2
  y_IEEE16d(k,:)=PL_IEEE80216d(fc,distance,'A',htx(k),hrx(k),'atnt');
  y_MIEEE16d(k,:)=PL_IEEE80216d(fc,distance,'A',htx(k),hrx(k),
      'atnt','mod');
end
subplot(121), semilogx(distance,y_IEEE16d(1,:),'k:','linewidth',1.5)
hold on, semilogx(distance,y_IEEE16d(2,:),'k-','linewidth',1.5)
```

```
grid on, axis([1 1000 10 150])
title(['IEEE 802.16d Path-loss Model, f_c=',num2str(fc/1e6),'MHz'])
xlabel('Distance[m]'), ylabel('Pathloss[dB]')
legend('h_{Tx}=30m, h_{Rx}=2m','h_{Tx}=30m, h_{Rx}=10m',2)
subplot(122), semilogx(distance,y_MIEEE16d(1,:),'k:','linewidth',1.5)
hold on, semilogx(distance,y_MIEEE16d(2,:),'k-','linewidth',1.5)
grid on, axis([1 1000 10 150])
title(['Modified IEEE 802.16d Path-loss Model, f_c=', num2str(fc/1e6), 'MHz'])
xlabel('Distance[m]'), ylabel('Pathloss[dB]')
legend('h_{Tx}=30m, h_{Rx}=2m','h_{Tx}=30m, h_{Rx}=10m',2)
```

1.2 Small-Scale Fading

Unless confused with large-scale fading, small-scale fading is often referred to as fading in short. Fading is the rapid variation of the received signal level in the short term as the user terminal moves a short distance. It is due to the effect of multiple signal paths, which cause interference when they arrive subsequently in the receive antenna with varying phases (i.e., constructive interference with the same phase and destructive interference with a different phase). In other words, the variation of the received signal level depends on the relationships of the relative phases among the number of signals reflected from the local scatters. Furthermore, each of the multiple signal paths may undergo changes that depend on the speeds of the mobile station and surrounding objects. In summary, small-scale fading is attributed to multi-path propagation, mobile speed, speed of surrounding objects, and transmission bandwidth of signal.

1.2.1 Parameters for Small-Scale Fading

Characteristics of a multipath fading channel are often specified by a power delay profile (PDP). Table 1.4 presents one particular example of PDP specified for the pedestrian channel model by ITU-R, in which four different multiple signal paths are characterized by their relative delay and average power. Here, the relative delay is an excess delay with respect to the reference time while average power for each path is normalized by that of the first path (tap) [12].

Table 1.4 Power delay profile: example (ITU-R Pedestrian A Model).

Tab	Relative delay (*ns*)	Average power (*dB*)
1	0	0.0
2	110	−9.7
3	190	−19.2
4	410	−22.8

Mean excess delay and *RMS delay spread* are useful channel parameters that provide a reference of comparison among the different multipath fading channels, and furthermore, show a general guideline to design a wireless transmission system. Let τ_k denote the channel delay of the kth path while a_k and $P(\tau_k)$ denote the amplitude and power, respectively. Then, the mean excess delay $\bar{\tau}$ is given by the first moment of PDP as

$$\bar{\tau} = \frac{\sum_k a_k^2 \tau_k}{\sum_k a_k^2} = \frac{\sum_k \tau_k P(\tau_k)}{\sum_k P(\tau_k)} \tag{1.19}$$

Meanwhile, RMS delay spread σ_τ is given by the square root of the second central moment of PDP as

$$\sigma_\tau = \sqrt{\overline{\tau^2} - (\bar{\tau})^2} \tag{1.20}$$

where

$$\overline{\tau^2} = \frac{\sum_k a_k^2 \tau_k^2}{\sum_k a_k^2} = \frac{\sum_k \tau_k^2 P(\tau_k)}{\sum_k P(\tau_k)} \tag{1.21}$$

In general, *coherence bandwidth*, denoted as B_c, is inversely-proportional to the RMS delay spread, that is,

$$B_c \approx \frac{1}{\sigma_\tau} \tag{1.22}$$

The relation in Equation (1.22) may vary with the definition of the coherence bandwidth. For example, in the case where the coherence bandwidth is defined as a bandwidth with correlation of 0.9 or above, coherence bandwidth and RMS delay spread are related as

$$B_c \approx \frac{1}{50\sigma_\tau} \tag{1.23}$$

In the case where the coherence bandwidth is defined as a bandwidth with correlation of 0.5 or above, it is given as

$$B_c \approx \frac{1}{5\sigma_\tau} \tag{1.24}$$

1.2.2 Time-Dispersive vs. Frequency-Dispersive Fading

As mobile terminal moves, the specific type of fading for the corresponding receiver depends on both the transmission scheme and channel characteristics. The transmission scheme is specified with signal parameters such as signal bandwidth and symbol period. Meanwhile, wireless channels can be characterized by two different channel parameters, multipath delay spread and Doppler spread, each of which causes time dispersion and frequency dispersion, respectively. Depending on the extent of time dispersion or frequency dispersion, the frequency-selective fading or time-selective fading is induced respectively.

1.2.2.1 Fading Due to Time Dispersion: Frequency-Selective Fading Channel

Due to time dispersion, a transmit signal may undergo fading over a frequency domain either in a selective or non-selective manner, which is referred to as *frequency-selective fading* or

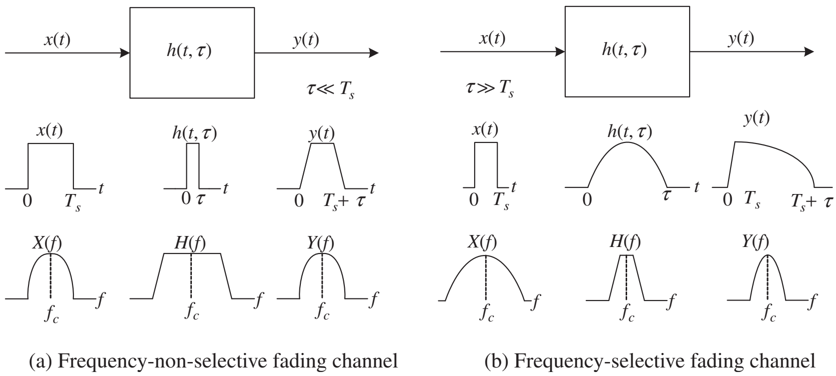

Figure 1.10 Characteristics of fading due to time dispersion over multi-path channel [2]. (Rappaport, Theodore S., *Wireless Communications: Principles and Practice*, 2nd Edition, © 2002, pgs. 130–131. Reprinted by permission of Pearson Education, Inc., Upper Saddle River, New Jersey.)

frequency-non-selective fading, respectively. For the given channel frequency response, frequency selectivity is generally governed by signal bandwidth. Figure 1.10 intuitively illustrates how channel characteristics are affected by the signal bandwidth in the frequency domain. Due to time dispersion according to multi-paths, channel response varies with frequency. Here, the transmitted signal is subject to frequency-non-selective fading when signal bandwidth is narrow enough such that it may be transmitted over the flat response. On the other hand, the signal is subject to frequency-selective fading when signal bandwidth is wide enough such that it may be filtered out by the finite channel bandwidth.

As shown in Figure 1.10(a), the received signal undergoes frequency-non-selective fading as long as the bandwidth of the wireless channel is wider than that of the signal bandwidth, while maintaining a constant amplitude and linear phase response within a passband. Constant amplitude undergone by signal bandwidth induces *flat fading*, which is another term to refer to frequency-non-selective fading. Here, a narrower bandwidth implies that symbol period T_s is greater than delay spread τ of the multipath channel $h(t, \tau)$. As long as T_s is greater than τ, the current symbol does not affect the subsequent symbol as much over the next symbol period, implying that inter-symbol interference (ISI) is not significant. Even while amplitude is slowly time-varying in the frequency-non-selective fading channel, it is often referred to as a narrowband channel, since the signal bandwidth is much narrower than the channel bandwidth. To summarize the observation above, a transmit signal is subject to frequency-non-selective fading under the following conditions:

$$B_s \ll B_c \quad \text{and} \quad T_s \gg \sigma_\tau \tag{1.25}$$

where B_s and T_s are the bandwidth and symbol period of the transmit signal, while B_c and σ_τ denote coherence bandwidth and RMS delay spread, respectively.

As mentioned earlier, transmit signal undergoes frequency-selective fading when the wireless channel has a constant amplitude and linear phase response only within a channel bandwidth narrower than the signal bandwidth. In this case, the channel impulse response has a larger delay spread than a symbol period of the transmit signal. Due to the short symbol duration as compared to the multipath delay spread, multiple-delayed copies of the transmit signal is significantly overlapped with the subsequent symbol, incurring inter-symbol interference (ISI). The term *frequency selective channel* is used simply because the amplitude of frequency response varies with the frequency, as opposed to the frequency-flat nature of the frequency-non-selective fading channel. As illustrated in Figure 1.10(b), the occurrence of ISI is obvious in the time domain since channel delay spread τ is much greater than the symbol period. This implies that signal bandwidth B_s is greater than coherence bandwidth B_c and thus, the received signal will have a different amplitude in the frequency response (i.e., undergo frequency-selective fading). Since signal bandwidth is larger than the bandwidth of channel impulse response in frequency-selective fading channel, it is often referred to as a wideband channel. To summarize the observation above, transmit signal is subject to frequency-selective fading under the following conditions:

$$B_s > B_c \quad \text{and} \quad T_s > \sigma_\tau \tag{1.26}$$

Even if it depends on modulation scheme, a channel is typically classified as frequency-selective when $\sigma_\tau > 0.1T_s$.

1.2.2.2 Fading Due to Frequency Dispersion: Time-Selective Fading Channel

Depending on the extent of the Doppler spread, the received signal undergoes fast or slow fading. In a *fast fading* channel, the coherence time is smaller than the symbol period and thus, a channel impulse response quickly varies within the symbol period. Variation in the time domain is closely related to movement of the transmitter or receiver, which incurs a spread in the frequency domain, known as a Doppler shift. Let f_m be the maximum Doppler shift. The bandwidth of Doppler spectrum, denoted as B_d, is given as $B_d = 2f_m$. In general, the *coherence time*, denoted as T_c, is inversely proportional to Doppler spread, i.e.,

$$T_c \approx \frac{1}{f_m} \tag{1.27}$$

Therefore, $T_s > T_c$ implies $B_s < B_d$. The transmit signal is subject to fast fading under the following conditions:

$$T_s > T_c \quad \text{and} \quad B_s < B_d \tag{1.28}$$

On the other hand, consider the case that channel impulse response varies slowly as compared to variation in the baseband transmit signal. In this case, we can assume that the channel does not change over the duration of one or more symbols and thus, it is referred to as a *static* channel. This implies that the Doppler spread is much smaller than the bandwidth of the baseband transmit signal. In conclusion, transmit signal is subject to slow fading under the following conditions:

$$T_s \ll T_c \quad \text{and} \quad B_s \gg B_d \tag{1.29}$$

In the case where the coherence time is defined as a bandwidth with the correlation of 0.5 or above [1], the relationship in Equation (1.27) must be changed to

$$T_c \approx \frac{9}{16\pi f_m} \tag{1.30}$$

Note that Equation (1.27) is derived under the assumption that a Rayleigh-faded signal varies very slowly, while Equation (1.30) is derived under the assumption that a signal varies very fast. The most common definition of coherence time is to use the geometric mean of Equation (1.27) and Equation (1.30) [1], which is given as

$$T_c = \sqrt{\frac{9}{16\pi f_m^2}} = \frac{0.423}{f_m} \tag{1.31}$$

It is important to note that fast or slow fading does not have anything to do with time dispersion-induced fading. In other words, the frequency selectivity of the wireless channel cannot be judged merely from the channel characteristics of fast or slow fading. This is simply because fast fading is attributed only to the rate of channel variation due to the terminal movement.

1.2.3 Statistical Characterization and Generation of Fading Channel

1.2.3.1 Statistical Characterization of Fading Channel

Statistical model of the fading channel is to Clarke's credit that he statistically characterized the electromagnetic field of the received signal at a moving terminal through a scattering process [12]. In Clarke's proposed model, there are N planewaves with arbitrary carrier phases, each coming from an arbitrary direction under the assumption that each planewave has the same average power [13–16].

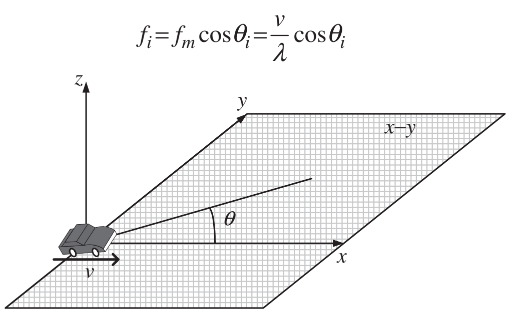

Figure 1.11 Planewave arriving at the receiver that moves in the direction of x with a velocity of v.

Figure 1.11 shows a planewave arriving from angle θ with respect to the direction of a terminal movement with a speed of v, where all waves are arriving from a horizontal direction on $x-y$ plane. As a mobile station moves, all planewaves arriving at the receiver undergo the Doppler shift. Let $x(t)$ be a baseband transmit signal. Then, the corresponding passband transmit signal is given as

$$\tilde{x}(t) = \mathrm{Re}\left[x(t)e^{j2\pi f_c t}\right] \tag{1.32}$$

where $\mathrm{Re}[s(t)]$ denotes a real component of $s(t)$. Passing through a scattered channel of I different propagation paths with different Doppler shifts, the passband received signal can be represented as

$$\begin{aligned}\tilde{y}(t) &= \mathrm{Re}\left[\sum_{i=1}^{I} C_i e^{j2\pi(f_c+f_i)(t-\tau_i)} x(t-\tau_i)\right] \\ &= \mathrm{Re}\left[y(t)e^{j2\pi f_c t}\right]\end{aligned} \tag{1.33}$$

where C_i, τ_i, and f_i denote the channel gain, delay, and Doppler shift for the ith propagation path, respectively. For the mobile speed of v and the wavelength of λ, Doppler shift is given as

$$f_i = f_m \cos\theta_i = \frac{v}{\lambda}\cos\theta_i \tag{1.34}$$

where f_m is the maximum Doppler shift and θ_i is the angle of arrival (AoA) for the ith planewave. Note that the baseband received signal in Equation (1.33) is given as

$$y(t) = \sum_{i=1}^{I} C_i e^{-j\phi_i(t)} x(t-\tau_i) \tag{1.35}$$

where $\phi_i(t) = 2\pi\{(f_c+f_i)\tau_i - f_i t_i\}$. According to Equation (1.35), therefore, the corresponding channel can be modeled as a linear time-varying filter with the following complex baseband impulse response:

$$h(t,\tau) = \sum_{i=1}^{I} C_i e^{-j\phi_i(t)} \delta(t-\tau_i) \tag{1.36}$$

where $\delta(\cdot)$ is a Dirac delta function. As long as difference in the path delay is much less than the sampling period T_S, path delay τ_i can be approximated as $\hat{\tau}$. Then, Equation (1.36) can be represented as

$$h(t,\tau) = h(t)\delta(t-\hat{\tau}) \tag{1.37}$$

where $h(t) = \sum_{i=1}^{I} C_i e^{-j\phi_i(t)}$. Assuming that $x(t) = 1$, the received passband signal $\tilde{y}(t)$ can be expressed as

$$\begin{aligned}\tilde{y}(t) &= \mathrm{Re}\left[y(t)e^{j2\pi f_c t}\right] \\ &= \mathrm{Re}\left[\{h_I(t) + jh_Q(t)\}e^{j2\pi f_c t}\right] \\ &= h_I(t)\cos 2\pi f_c t - h_Q(t)\sin 2\pi f_c t\end{aligned} \tag{1.38}$$

where $h_I(t)$ and $h_Q(t)$ are in-phase and quadrature components of $h(t)$, respectively given as

$$h_I(t) = \sum_{i=1}^{I} C_i \cos\phi_i(t) \tag{1.39}$$

and

$$h_Q(t) = \sum_{i=1}^{I} C_i \sin\phi_i(t) \tag{1.40}$$

Assuming that I is large enough, $h_I(t)$ and $h_Q(t)$ in Equation (1.39) and Equation (1.40) can be approximated as Gaussian random variables by the central limit theorem. Therefore, we conclude that the amplitude of the received signal, $\tilde{y}(t) = \sqrt{h_I^2(t) + h_Q^2(t)}$, over the multipath channel subject to numerous scattering components, follows the Rayleigh distribution. The power spectrum density (PSD) of the fading process is found by the Fourier transform of the autocorrelation function of $\tilde{y}(t)$and is given by [12]

$$S_{\tilde{y}\tilde{y}}(f) = \begin{cases} \dfrac{\Omega_p}{4\pi f_m} \dfrac{1}{\sqrt{1 - \left(\dfrac{f - f_c}{f_m}\right)^2}} & |f - f_c| \le f_m \\ 0 & \text{otherwise} \end{cases} \tag{1.41}$$

where $\Omega_p = E\{h_I^2(t)\} + E\{h_Q^2(t)\} = \sum_{i=1}^{I} C_i^2$. The power spectrum density in Equation (1.41) is often referred to as the *classical Doppler spectrum*.

Meanwhile, if some of the scattering components are much stronger than most of the components, the fading process no longer follows the Rayleigh distribution. In this case, the amplitude of the received signal, $\tilde{y}(t) = \sqrt{h_I^2(t) + h_Q^2(t)}$, follows the Rician distribution and thus, this fading process is referred to as *Rician fading*.

The strongest scattering component usually corresponds to the *line-of-sight* (LOS) component (also referred to as *specular* components). Other than the LOS component, all the other components are non-line-of-sight (NLOS) components (referred to as *scattering* components). Let $\tilde{p}(\theta)$ denote a probability density function (PDF) of AoA for the scattering components and θ_0 denote AoA for the specular component. Then, the PDF of AoA for all components is given as

$$p(\theta) = \frac{1}{K+1}\tilde{p}(\theta) + \frac{K}{K+1}\delta(\theta - \theta_0) \tag{1.42}$$

where K is the Rician factor, defined as a ratio of the specular component power c^2 and scattering component power $2\sigma^2$, shown as

$$K = \frac{c^2}{2\sigma^2} \tag{1.43}$$

In the subsequent section, we discuss how to compute the probability density of the above fading processes, which facilitate generating Rayleigh fading and Rician fading.

1.2.3.2 Generation of Fading Channels

In general, the propagation environment for any wireless channel in either indoor or outdoor may be subject to LOS (Line-of-Sight) or NLOS (Non Line-of-Sight). As described in the previous subsection, a probability density function of the signal received in the LOS environment follows the Rician distribution, while that in the NLOS environment follows the

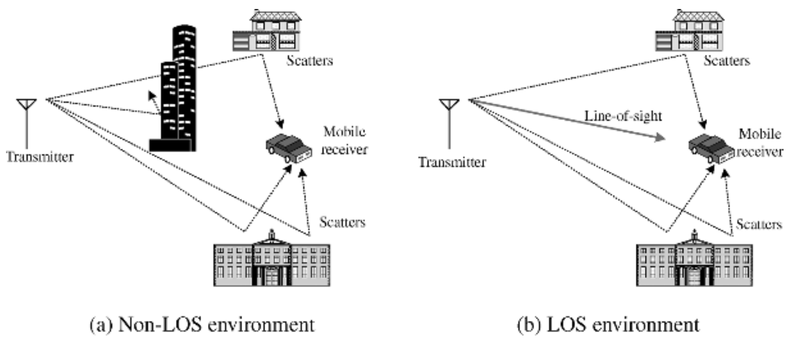

Figure 1.12 Non-LOS and LOS propagation environments.

Rayleigh distribution. Figure 1.12 illustrates these two different environments: one for LOS and the other for NLOS.

Note that any received signal in the propagation environment for a wireless channel can be considered as the sum of the received signals from an infinite number of scatters. By the central limit theorem, the received signal can be represented by a Gaussian random variable. In other words, a wireless channel subject to the fading environments in Figure 1.12 can be represented by a complex Gaussian random variable, $W_1 + jW_2$, where W_1 and W_2 are the independent and identically-distributed (i.i.d.) Gaussian random variables with a zero mean and variance of σ^2. Let X denote the amplitude of the complex Gaussian random variable $W_1 + jW_2$, such that $X = \sqrt{W_1^2 + W_2^2}$. Then, note that X is a Rayleigh random variable with the following probability density function (PDF):

$$f_X(x) = \frac{x}{\sigma^2} e^{-\frac{x^2}{2\sigma^2}} \tag{1.44}$$

where $2\sigma^2 = E\{X^2\}$. Furthermore, X^2 is known as a chi-square (χ^2) random variable.

Below, we will discuss how to generate the Rayleigh random variable X. First of all, we generate two i.i.d. Gaussian random variables with a zero mean and unit variance, Z_1 and Z_2, by using a built-in MATLAB® function, "randn." Note that the Rayleigh random variable X with the PDF in Equation (1.44) can be represented by

$$X = \sigma \cdot \sqrt{Z_1^2 + Z_2^2} \tag{1.45}$$

where $Z_1 \sim \mathcal{N}(0,1)$ and $Z_2 \sim \mathcal{N}(0,1)$[1]. Once Z_1 and Z_2 are generated by the built-in function "randn," the Rayleigh random variable X with the average power of $E\{X^2\} = 2\sigma^2$ can be generated by Equation (1.45).

In the line-of-sight (LOS) environment where there exists a strong path which is not subject to any loss due to reflection, diffraction, and scattering, the amplitude of the received signal can be expressed as $X = c + W_1 + jW_2$ where c represents the LOS component while W_1 and W_2 are the i.i.d. Gaussian random variables with a zero mean and variance of σ^2 as in the non-LOS environment. It has been known that X is the Rician random variable with the

[1] $\mathcal{N}(m,\sigma^2)$ represents a Gaussian (normal) distribution with a mean of m and variance of σ^2.

following PDF:

$$f_X(x) = \frac{x}{\sigma^2} e^{-\frac{x^2+c^2}{2\sigma^2}} I_0\left(\frac{xc}{\sigma^2}\right) \tag{1.46}$$

where $I_0(\cdot)$ is the modified zeroth-order Bessel function of the first kind. Note that Equation (1.46) can be represented in terms of the Rician K-factor defined in Equation (1.43). In case that there does exist an LOS component (i.e., $K=0$), Equation (1.46) reduces to the Rayleigh PDF Equation (1.44) as in the non-LOS environment. As K increases, Equation (1.46) tends to be the Gaussian PDF. Generally, it is assumed that $K \sim -40$dB for the Rayleigh fading channel and $K > 15$dB for the Gaussian channel. In the LOS environment, the first path that usually arrives with any reflection can be modeled as a Rician fading channel.

Figure 1.13 has been produced by running Program 1.8 ("plot_Ray_Ric_channel.m"), which calls Program 1.9 ("Ray_model") and Program 1.10 ("Ric_model") to generate the Rayleigh fading and Rician fading channels, respectively. It also demonstrates that the Rician distribution approaches Rayleigh distribution and Gaussian distribution when $K=-40$dB and $K=15$dB, respectively.

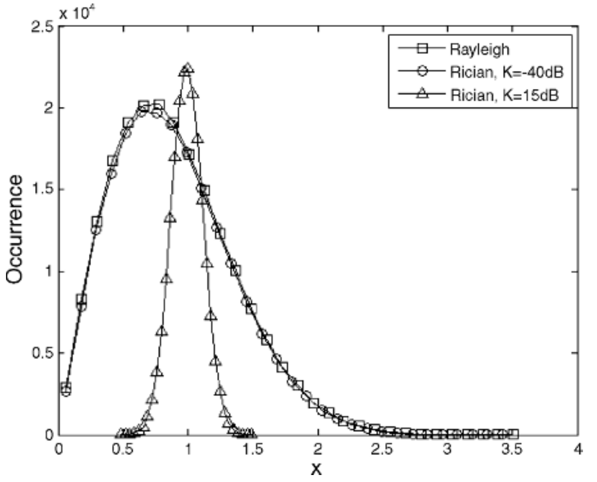

Figure 1.13 Distributions for Rayleigh and Rician fading channels.

Refer to [17–22] for additional information about propagation and fading in wireless channels.

MATLAB® Programs: Rayleigh Fading and Rician Fading Channels

Program 1.8 "plot_Ray_Ric_channel.m" to generate Rayleigh and Rician fading channels

```
% plot_Ray_Ric_channel.m
clear, clf
N=200000; level=30; K_dB=[-40 15];
gss=['k-s'; 'b-o'; 'r-^'];
% Rayleigh model
```

```
Rayleigh_ch=Ray_model(N);
[temp,x]=hist(abs(Rayleigh_ch(1,:)),level);
plot(x,temp,gss(1,:)), hold on
% Rician model
for i=1:length(K_dB);
  Rician_ch(i,:) = Ric_model(K_dB(i),N);
  [temp x] = hist(abs(Rician_ch(i,:)),level);
  plot(x,temp,gss(i+1,:))
end
xlabel('x'), ylabel('Occurrence')
legend('Rayleigh','Rician, K=-40dB','Rician, K=15dB')
```

Program 1.9 "Ray_model" for Rayleigh fading channel model

```
function H=Ray_model(L)
% Rayleigh channel model
% Input : L = Number of channel realizations
% Output: H = Channel vector
H = (randn(1,L)+j*randn(1,L))/sqrt(2);
```

Program 1.10 "Ric_model" for Rician fading channel model

```
function H=Ric_model(K_dB,L)
% Rician channel model
% Input : K_dB = K factor[dB]
% Output: H = Channel vector
K = 10^(K_dB/10);
H = sqrt(K/(K+1)) + sqrt(1/(K+1))*Ray_model(L);
```